

Inclusive $\bar{B} \rightarrow X_s \ell^+ \ell^-$ at the LHC: theory predictions and new-physics reach

Tobias Huber¹, Tobias Hurth², Jack Jenkins¹, Enrico Lunghi³, Qin Qin⁴, K. Keri Vos^{5,6}

¹*Theoretische Physik 1, Center for Particle Physics Siegen (CPPS), Universität Siegen, Walter-Flex-Straße 3, D-57068 Siegen, Germany*

²*PRISMA+ Cluster of Excellence and Institute for Physics (THEP), Johannes Gutenberg University, D-55099 Mainz, Germany*

³*Physics Department, Indiana University, Bloomington, IN 47405, USA*

⁴*School of Physics, Huazhong University of Science and Technology, Wuhan 430074, China*

⁵*Gravitational Waves and Fundamental Physics (GWFP), Maastricht University, Duboisdomein 30, NL-6229 GT Maastricht, the Netherlands*

⁶*Nikhef, Science Park 105, NL-1098 XG Amsterdam, the Netherlands*

E-mail: huber@physik.uni-siegen.de, tobias.hurth@cern.ch,
jack.jenkins@uni-siegen.de, elunghi@iu.edu, qqin@hust.edu.cn,
k.vos@maastrichtuniversity.nl

ABSTRACT: We present theoretical predictions for observables in inclusive $\bar{B} \rightarrow X_s \ell^+ \ell^-$ suitable for measurements at hadron colliders through a sum-over-exclusive approach. At low q^2 we calculate the branching ratio and three angular observables. At high q^2 we provide the branching ratio and the ratio of the $\bar{B} \rightarrow X_s \ell^+ \ell^-$ rate with respect to the inclusive $\bar{B} \rightarrow X_u \ell \bar{\nu}$ rate with the same phase-space cut. We compare our predictions to an extraction of the experimental rate through a sum-over-exclusive method using branching ratios of the exclusive $\bar{B} \rightarrow K^{(*)} \mu^+ \mu^-$ modes measured at LHCb. Our analysis does not support a recent claim about a deficit in the inclusive branching ratio in the high- q^2 region. Finally, we present current model-independent bounds on new physics and emphasize the potential of complementary analyses of $\bar{B} \rightarrow X_s \ell^+ \ell^-$ at Belle II and the LHC.

KEYWORDS: B-physics, Rare Decays, Physics Beyond the Standard Model

Contents

1	Introduction	1
2	Input parameters	3
3	Phenomenological results	4
3.1	Standard Model predictions for LHCb	4
3.2	Comparison with semi-inclusive measurements	7
3.3	Averaging experimental and theoretical results	9
4	New physics sensitivities	11
5	Conclusion	14
A	Standard Model predictions for the B factories	16

1 Introduction

Flavour-changing neutral transitions of heavy quarks remain prime candidates in the search for physics beyond the Standard Model (SM) of particle physics. In the exclusive $b \rightarrow s$ modes, such as $B \rightarrow K^{(*)} \ell^+ \ell^-$, several deviations between SM predictions and experimental measurements have been found. Theoretically, these predictions are challenging due to nonperturbative charm-loop effects, making a crosscheck via the inclusive modes indispensable and important [1–4].

Recently, a measurement of the inclusive $\bar{B} \rightarrow X_s \ell^+ \ell^-$ at LHCb using isospin symmetry has been proposed [5]. Such a measurement at a hadron collider is challenging and has to rely on the semi-inclusive method (sum over exclusive modes). In fact, also at Belle II there will first be a semi-inclusive measurement before a fully inclusive measurement using the recoil technique might become feasible.

In this letter, we present the corresponding theory predictions, adjusting previous predictions for $\bar{B} \rightarrow X_s \ell^+ \ell^-$ observables in the low- and also in the high- q^2 region¹ at Belle II [6–9] to the environment of the LHC. Specifically, in our previous calculations tailored for the Belle II experiment, we have included the logarithmically enhanced effects of a single-photon emission from the final state leptons in the collinear approximation. This collinear radiation does not affect the rate integrated over the full phase space, but should be taken into account when only parts of the phase space are considered (see Ref. [8], and Ref. [10] for $\bar{B} \rightarrow X_c \ell \bar{\nu}$). However, for a future LHCb analysis, such an effect should not be

¹Throughout the paper, q^2 denotes the di-lepton invariant mass squared.

included on the theory side as it is already subtracted using the PHOTOS software², see also the discussions in Ref. [11–13] for the exclusive $B \rightarrow K$ mode. Therefore, we present here our results without these collinear QED logarithms.

The theoretical description of the $\bar{B} \rightarrow X_s \ell^+ \ell^-$ decay includes NNLO QCD [14–22], NLO electroweak corrections [6–8, 23], and $1/m_b^2$ [24–27] and $1/m_b^3$ [28, 29] power-corrections. The five-particle contributions to $\bar{B} \rightarrow X_s \ell^+ \ell^-$ are numerically negligible [30]. Long-distance off-shell effects from intermediate charmonium resonances are included through the Krüger-Sehgal (KS) approach [31, 32] and the $1/m_c^2$ corrections [33] (see also the detailed discussions in Refs. [20, 34])³. We also mention here that in the low- q^2 region the local $1/m_c^2$ corrections get overwritten by the resolved (non-local) contributions [35–37] and should be replaced by the latter.

In the high- q^2 region, theoretical predictions of the branching ratio are very sensitive to power corrections arising in the employed operator-product expansion (OPE) framework. In addition, four-quark operators enter at order $1/m_b^3$ and higher. In order to reduce the sensitivity to these power corrections, it is interesting to consider the ratio [29]⁴

$$\mathcal{R}(q_0^2) = \int_{q_0^2}^{M_B^2} dq^2 \frac{d\Gamma(\bar{B} \rightarrow X_s \ell^+ \ell^-)}{dq^2} \bigg/ \int_{q_0^2}^{M_B^2} dq^2 \frac{d\Gamma(\bar{B} \rightarrow X_u \ell \bar{\nu})}{dq^2}, \quad (1.1)$$

where both the $b \rightarrow s$ and $b \rightarrow u$ decays have the same lower cut q_0^2 . In the low- q^2 region the ratio \mathcal{R} has reduced sensitivity to the hadronic mass cut which disrupts the local OPE [38–40]. We note that in this ratio, we should also consider the treatment of the log-enhanced QED terms in the $b \rightarrow u$ transition. After considering the experimental setup, we should not include such terms⁵. Hence, we present new calculations of this ratio, without log-enhanced QED corrections in both the $b \rightarrow u$ and $b \rightarrow s$ mode.

Finally, we study constraints on new physics from $\bar{B} \rightarrow X_s \ell^+ \ell^-$ in the high- and low- q^2 regions. The new-physics reach is strengthened by the interplay between (semi)-inclusive analyses at e^+e^- and hadron machines, and between inclusive and exclusive modes.

This article is organised as follows. We present our updated input parameters in section 2, which lead to our phenomenological results which we present in section 3. Here we also discuss the comparison between the direct calculation of the high- q^2 branching ratio in the OPE, versus that obtained through \mathcal{R} in (1.1) multiplied by the experimental results for the $\bar{B} \rightarrow X_u \ell \bar{\nu}$ decay. Moreover, we perform a comparison to several semi-inclusive measurements at high q^2 . We also comment on a recent calculation of \mathcal{R} , and critically reassess a claim about a deficit in the data within the high- q^2 region [41]. In section 4, we present our analysis of the new-physics reach, while we conclude in section 5. Additional numerical results including log-enhanced QED corrections are relegated to appendix A.

²We thank Patrick Owen, Ulrik Egede and Johannes Albrecht for discussions on this point.

³In this way there is no double counting within the off-shell effects of the resonances. While the KS method is exact when only factorisable contributions are taken into account, this means that the $\bar{B} \rightarrow X_s c \bar{c}$ transition can be factorised into the product of $\bar{s}b$ and $c\bar{c}$ colour singlet currents, the $1/m_c^2$ corrections represent the nonfactorisable $c\bar{c}$ long distance effects far from the resonances [20, 34]

⁴In this ratio, the nonperturbative corrections related to the dominant Q_9 and Q_{10} operators cancel out.

⁵We thank Florian Bernlochner and Lu Cao for discussions on this point.

2 Input parameters

In the high- q^2 region, the uncertainties of both the branching ratio \mathcal{B} and the ratio \mathcal{R} are dominated by power corrections to the OPE proportional to λ_i and ρ_i as defined in our previous work [9, 34]. The expressions of these observables with the heavy-quark expansion (HQE) parameters left symbolic are

$$\mathcal{B}[> 14.4] = (3.05 - 5.87 \lambda_2^{\text{eff}} + 8.09 \rho_1) \times 10^{-7}, \quad (2.1)$$

$$\mathcal{B}[> 15] = (2.55 - 5.717 \lambda_2^{\text{eff}} + 8.47 \rho_1) \times 10^{-7}, \quad (2.2)$$

$$\mathcal{R}(14.4) = (24.90 + 0.04 \lambda_1 + 2.49 \lambda_2^{\text{eff}} + 10.72 \rho_1) \times 10^{-4}, \quad (2.3)$$

$$\mathcal{R}(15) = (25.65 + 0.03 \lambda_1 + 3.66 \lambda_2^{\text{eff}} + 11.94 \rho_1) \times 10^{-4}, \quad (2.4)$$

where

$$\lambda_2^{\text{eff}} = \lambda_2 - \frac{\rho_2}{m_b}. \quad (2.5)$$

Here, the numerical values for λ_1 and λ_2^{eff} have to be inserted in units of GeV^2 , that of ρ_1 in units of GeV^3 . The effect of λ_2^{eff} and in particular ρ_1 is pronounced, and the dependence of the branching ratio on the HQE parameters is larger compared to the ratio \mathcal{R} [29]. The dependence of the branching ratios on λ_1 is marginal and not given separately. In addition, the effect of four-quark operators [29, 34, 42, 43] is large, but we do not give their dependence here explicitly.

In this chapter we update the values for the HQE parameters $\lambda_{1,2}$ and ρ_1 . All remaining input parameters are the same as in table 1 of Ref. [9]. The HQE parameters are extracted from the $\bar{B} \rightarrow X_c \ell \bar{\nu}$ spectrum. We use the results from Ref. [44], which defines the HQE elements for the physical states. A first analysis using only di-lepton invariant mass moments has also become available [45], which uses the reparametrization invariant basis [46] and includes also higher-order HQE elements. Very recently, also a new analysis appeared including all available moments of the spectrum [47]. The latter results are in agreement with the results in Ref. [44], which we use in our analysis.

As is by now customary, the HQE parameters are extracted in the kinetic scheme [48, 49] at a scale $\mu = 1 \text{ GeV}$. While for the b quark mass, we work in the 1S scheme as previously, we use the kinetic scheme for the HQE power corrections. To do so, it requires transforming from the pole scheme expression in Eq. (2.1) to the kinetic scheme using the perturbative corrections at the appropriate order (see e.g. Refs. [50, 51] and Ref. [52] for the recent update to $\mathcal{O}(\alpha_s^3)$). Since we work at NNLO, we apply only the $\mathcal{O}(\alpha_s^2)$ perturbative corrections. As previously, we convert the HQE parameters in the kinetic scheme to their pole scheme counterparts. Using the $\rho_D^3(\mu = 1 \text{ GeV})$ and $\mu_\pi^2(\mu = 1 \text{ GeV})$ values from [44], we then find

$$\rho_1 = \rho_D^3(0) = (0.080 \pm 0.031) \text{ GeV}^3, \quad -\lambda_1 = \mu_\pi^2(0) = (0.314 \pm 0.056) \text{ GeV}^2, \quad (2.6)$$

where contrary to the analysis in Ref. [34], we do not add an additional uncertainty due to missing higher orders. In addition, we have

$$\lambda_2^{\text{eff}} = \frac{\mu_G^2}{3} - \frac{\rho_{LS}^3}{m_b} = (0.111 \pm 0.018) \text{ GeV}^2 \quad (2.7)$$

where μ_G^2 and ρ_{LS}^3 do not receive any perturbative corrections when changing from the pole to the kinetic scheme or vice versa.

Besides, also four-quark operators (weak annihilation matrix elements) enter. Following the definitions in Refs. [9, 34], we stress again that the ratio \mathcal{R} is rather insensitive to these corrections and only depends on $f_s(f_{\text{NV}})$ and δf , which measures the SU(3) breaking between the strange and u four-quark operators. On the other hand, the branching ratio depends on both f_{NV} and f_{V} , the non-valence and valence weak annihilation contributions, respectively, which have a large uncertainty. We do not update these values here and use those given in Refs. [9, 34].

Finally, we note that in [9, 34] the branching ratio (and other angular observables) were obtained by normalizing to the ratio

$$C \equiv \left| \frac{V_{ub}}{V_{cb}} \right|^2 \frac{\Gamma(\bar{B} \rightarrow X_c e \bar{\nu})}{\Gamma(\bar{B} \rightarrow X_u e \bar{\nu})} \quad (2.8)$$

to suppress the weak annihilation contributions which enter both the neutral-current $\bar{B} \rightarrow X_s \ell^+ \ell^-$ and the charged-current $\bar{B} \rightarrow X_u \ell \bar{\nu}$ modes. Here we treat C as an input, which we take as in Ref. [9] although in principle this parameter will have shifted due to the updated power correction parameters (and higher-order α_s^3 corrections now available [53, 54]). In a future analysis, it may be interesting to reconsider this normalization channel.

3 Phenomenological results

3.1 Standard Model predictions for LHCb

As outlined in the introduction, we calculate the SM predictions for inclusive $\bar{B} \rightarrow X_s \ell^+ \ell^-$ without logarithmically enhanced electromagnetic corrections, to match the LHCb conditions. We give the branching ratio and $\mathcal{R}(q_0^2)$ in the high- q^2 region above $q_0^2 = 14.4$ and 15.0 GeV^2 . In the low- q^2 region, from $1 \text{ GeV}^2 < q^2 < 6 \text{ GeV}^2$, we present the branching ratio as well as the angular coefficients $\mathcal{H}_T, \mathcal{H}_L$ and \mathcal{H}_A defined in Refs. [8, 9]. These numbers (except for the $q^2 > 15 \text{ GeV}^2$ observables) were already given in Table 5 of Ref. [9], albeit without uncertainties. In Table 1, we give these observables and those for $q^2 > 15 \text{ GeV}^2$ for our updated input parameters and including uncertainties. In the low- q^2 region, the dominant contributions to the uncertainties stem from the resolved contribution [35–37] (5% of the total) and the renormalisation scale (around 3%).

In the high- q^2 region, we also provide below the numbers for the integrated branching ratio for two different values of the lower q^2 -cutoff and with individual uncertainties. The total uncertainty is obtained by combining the individual ones in quadrature.

q^2 range [GeV ²]	[1, 6]	[1, 3.5]	[3.5, 6]
\mathcal{B} [10 ⁻⁷]	16.87 ± 1.25	9.17 ± 0.61	7.70 ± 0.65
\mathcal{H}_T [10 ⁻⁷]	3.14 ± 0.25	1.49 ± 0.09	1.65 ± 0.17
\mathcal{H}_L [10 ⁻⁷]	13.65 ± 1.00	7.63 ± 0.54	6.02 ± 0.49
\mathcal{H}_A [10 ⁻⁷]	-0.27 ± 0.21	-1.08 ± 0.08	0.81 ± 0.16
q^2 range [GeV ²]	> 14.4	> 15	
\mathcal{B} [10 ⁻⁷]	3.04 ± 0.69	2.59 ± 0.68	
$\mathcal{R}(q_0^2)$ [10 ⁻⁴]	26.02 ± 1.76	27.00 ± 1.94	

Table 1: Phenomenological results without logarithmically enhanced electromagnetic effects. The slight changes compared to [9] are due to the change in the input parameters.

$$\begin{aligned}
\mathcal{B}[> 14.4] &= (3.04 \pm 0.25_{\text{scale}} \pm 0.03_{m_t} \pm 0.04_{C,m_c} \pm 0.22_{m_b} \pm 0.005_{\alpha_s} \pm 0.003_{\text{CKM}} \\
&\quad \pm 0.05_{\text{BR}_{s1}} \pm 0.25_{\rho_1} \pm 0.11_{\lambda_2} \pm 0.54_{f_{u,s}}) \times 10^{-7} \\
&= (3.04 \pm 0.69) \times 10^{-7}, \tag{3.1}
\end{aligned}$$

$$\begin{aligned}
\mathcal{B}[> 15] &= (2.59 \pm 0.21_{\text{scale}} \pm 0.03_{m_t} \pm 0.05_{C,m_c} \pm 0.19_{m_b} \pm 0.004_{\alpha_s} \pm 0.002_{\text{CKM}} \\
&\quad \pm 0.04_{\text{BR}_{s1}} \pm 0.26_{\rho_1} \pm 0.10_{\lambda_2} \pm 0.54_{f_{u,s}}) \times 10^{-7} \\
&= (2.59 \pm 0.68) \times 10^{-7}. \tag{3.2}
\end{aligned}$$

We note that the uncertainty is dominated by the uncertainty on the higher-order HQE parameters and four-quark operators, and could be reduced with improved inputs. Moreover, we observe that the branching ratio drops rather steeply as the lower q^2 -cutoff is increased. The branching ratio is $\sim 15\%$ smaller when integrating from 15 GeV² compared to 14.4 GeV². Hence both, from the point of view of statistics, and on theoretical grounds a lower cutoff $q_0^2 = 14.4$ GeV² is favourable. In the high- q^2 region, one encounters a breakdown of the heavy-mass expansion at the endpoint of the spectrum. However, for an *integrated* spectrum an effective expansion in inverse powers of $m_b^{\text{eff}} = m_b(1 - \sqrt{q_0^2/m_b^2})$ rather than m_b is found [20, 27, 55, 56], which is expected to behave better the lower q_0^2 is.

Alternatively, we can calculate the ratio $\mathcal{R}(q_0^2)$ defined in Eq. (1.1), which has a reduced sensitivity to the power corrections. Excluding logarithmically enhanced electromagnetic corrections in both the $b \rightarrow s$ and $b \rightarrow u$ transition, we obtain

$$\begin{aligned}
\mathcal{R}(14.4) &= (26.02 \pm 0.42_{\text{scale}} \pm 0.30_{m_t} \pm 0.11_{C,m_c} \pm 0.10_{m_b} \pm 0.12_{\alpha_s} \pm 1.12_{\text{CKM}} \\
&\quad \pm 0.33_{\rho_1} \pm 0.05_{\lambda_2} \pm 1.20_{f_{u,s}}) \times 10^{-4} \\
&= (26.02 \pm 1.76) \times 10^{-4}, \tag{3.3}
\end{aligned}$$

$$\begin{aligned}
\mathcal{R}(15) &= (27.00 \pm 0.25_{\text{scale}} \pm 0.30_{m_t} \pm 0.11_{C,m_c} \pm 0.17_{m_b} \pm 0.15_{\alpha_s} \pm 1.16_{\text{CKM}} \\
&\quad \pm 0.37_{\rho_1} \pm 0.07_{\lambda_2} \pm 1.43_{f_{u,s}}) \times 10^{-4} \\
&= (27.00 \pm 1.94) \times 10^{-4}.
\end{aligned} \tag{3.4}$$

We can now use the \mathcal{R} ratio combined with the latest Belle measurement of the inclusive branching ratio $\mathcal{B}(\bar{B} \rightarrow X_u \ell \bar{\nu})$ [57] to obtain the inclusive branching ratio $\mathcal{B}(\bar{B} \rightarrow X_s \ell^+ \ell^-)$ [41]. From Ref. [57]⁶, we find

$$\mathcal{B}(\bar{B} \rightarrow X_u \ell \bar{\nu})[> 14.4]_{\text{exp}} = (1.76 \pm 0.32) \times 10^{-4}, \tag{3.5}$$

$$\mathcal{B}(\bar{B} \rightarrow X_u \ell \bar{\nu})[> 15]_{\text{exp}} = (1.52 \pm 0.28) \times 10^{-4}, \tag{3.6}$$

where the latter is in agreement with the value quoted in Ref. [41]. Using now our theoretical prediction for the ratio \mathcal{R} , we find

$$\begin{aligned}
\mathcal{B}[> 14.4]_{\text{SM},\mathcal{R}} &= \mathcal{R}(14.4) \times \mathcal{B}(B \rightarrow X_u \ell \bar{\nu})[> 14.4]_{\text{exp}} \\
&= (4.58 \pm 0.89) \times 10^{-7}.
\end{aligned} \tag{3.7}$$

$$\begin{aligned}
\mathcal{B}[> 15]_{\text{SM},\mathcal{R}} &= \mathcal{R}(15) \times \mathcal{B}(B \rightarrow X_u \ell \bar{\nu})[> 15]_{\text{exp}} \\
&= (4.10 \pm 0.81) \times 10^{-7}.
\end{aligned} \tag{3.8}$$

These determinations are compatible with our direct calculations in Eqs. (3.1) and (3.2). The comparison between the two values is given in Figure 1. It will be interesting to see how the central value of $\mathcal{B}(\bar{B} \rightarrow X_u \ell \bar{\nu})$ will develop in the future with more statistics. Also the power corrections in the branching ratios of Eqs. (3.1) and (3.2) will be scrutinized in the future.

Finally, let us briefly comment on the prediction of the ratio \mathcal{R} in Ref. [41]. The authors find a larger central value and also a larger uncertainty compared to our prediction. To further analyse this issue, we divide our central value $\mathcal{R}(15) = 0.0027$ by the ratio $|V_{tb}V_{ts}^*/V_{ub}|^2 = 123.5$ of CKM elements (see Table 1 of Ref. [9]), and obtain a value of 2.19×10^{-5} , which turns out to be 13% smaller than the central value 2.51×10^{-5} obtained from Eq. (22) in Ref. [41]. The difference can be traced back to the fact that we include the two-loop $\mathcal{O}(\alpha_s^2)$ -corrections induced by the mixing of current-current operators into Q_7 and Q_9 [20–22, 58], as well as the factorisable $c\bar{c}$ long distance off-shell effects via the KS-approach [31, 32]. Both contributions seem to be absent in the analysis of Ref. [41] – which largely relies on the implementation in Ref. [29] – and result in a correction in the same direction.

Adding the effect of the $Q_{1,2} - Q_{7,9}$ interference at order $\mathcal{O}(\alpha_s^2)$ shifts $\mathcal{R}(15)$ by $\sim -9\%$, which reveals that this is the main source of discrepancy with our result. The remaining difference can be attributed to the factorisable $c\bar{c}$ long distance off-shell effects via the KS-approach; adding the latter contribution leads to an additional shift of $\mathcal{R}(15)$ by $\sim -4\%$. When adding these two contributions to the result in Eq. (22) of Ref. [41], we still find a small difference at the one-percent level with our result. We conjecture that the

⁶This result was obtained using the q^2 differential data provided by the Belle II collaboration in <https://doi.org/10.17182/hepdata.131599>

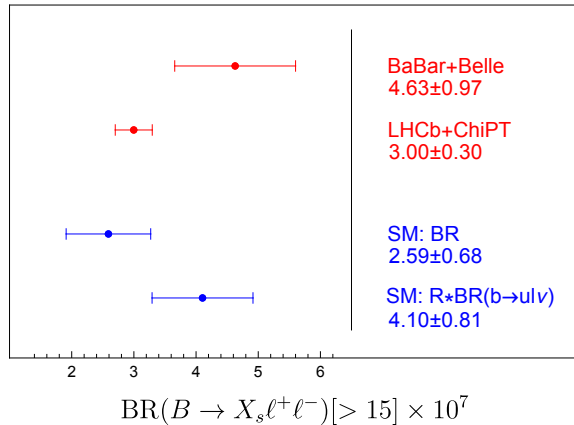


Figure 1: Comparison between the high- q^2 branching ratio obtained from BaBar and Belle in (3.11) and a sum over exclusive states using LHCb data and the ChiPT estimate from [41] given in (3.10). In addition, we show the direct SM theory prediction in (3.2) and that obtained by multiplying the ratio \mathcal{R} by the experimental $\bar{B} \rightarrow X_u \ell \bar{\nu}$ rate from (3.8).

tiny difference originates from different input parameters and the fact that the authors of Ref. [41] implement the full NLO electroweak matching at the high scale [59], while our code contains this contribution only in the large- m_t limit (see Ref. [60] and references therein).

As stated earlier, it is unarguable that the two-loop QCD matrix elements of the $Q_{1,2} - Q_{7,9}$ interference [20] must be included, as well as the long-distance off-shell effects from the intermediate charmonium resonances, the factorisable ones via the KS approach [31, 32] and the nonfactorisable ones via $1/m_c^2$ corrections [33] (see also discussions in Refs. [20, 34]).

3.2 Comparison with semi-inclusive measurements

Recently, the authors of Ref. [41] constructed a semi-inclusive experimental determination of $\bar{B} \rightarrow X_s \ell^+ \ell^-$ in the high- q^2 region. In this region, the semi-inclusive measurement is relatively simple because the rate is dominated by a limited number of exclusive modes. In the new analysis [41], the previously known prediction of non-resonant $K\pi$ states in the high- q^2 region of Ref. [27] – based on heavy hadron chiral perturbation theory (ChiPT) – was updated and the authors argued that above $q_0^2 = 15 \text{ GeV}^2$ the inclusive rate is dominated by the $B \rightarrow K$, $B \rightarrow K^*$ and $B \rightarrow K\pi$ modes. Modes with three final-state hadrons were neglected due to the highly suppressed phase space.

By combining the experimental LHCb measurements of the two dominant $B^+ \rightarrow K^+$ and $B^+ \rightarrow K^{*+}$ modes [61] and the update of the non-resonant $K\pi$ states, the authors of Ref. [41] found $\mathcal{B}[> 15]_{\text{LHCb+ChiPT}}^{\text{charged only}} = (2.74 \pm 0.41) \times 10^{-7}$ for the semi-inclusive branching ratio in the high- q^2 region. In this procedure, the ChiPT contribution was included by first normalizing it to the $B \rightarrow K$ and $B \rightarrow K^*$ theory inputs in the high- q^2 region, see Eq. (38)

in [41]. Adding instead the ChiPT contribution given in Eq. (34)⁷ of Ref. [41] directly to the sum of exclusive modes, we find

$$\mathcal{B}[> 15]_{\text{LHCb+ChiPT}}^{\text{charged only}} = (3.01 \pm 0.43) \times 10^{-7}. \quad (3.9)$$

We note that the corresponding neutral modes $B^0 \rightarrow K^0$ and $B^0 \rightarrow K^{*0}$ are also available [61, 62]. Forming the isospin average shifts the central value marginally but reduces the uncertainty of the sum of the two modes, and yields

$$\mathcal{B}[> 15]_{\text{LHCb+ChiPT}} = (3.00 \pm 0.30) \times 10^{-7}. \quad (3.10)$$

Comparing Eq. (3.10) to our theory prediction of the branching ratio in the same region in (3.2), we find good agreement. We note that the uncertainty on the theoretical predictions is twice as large as the estimated uncertainty given in Eq. (3.10). Comparing to the value extracted using \mathcal{R} in Eq. (3.8), we also find compatibility with the experimental result in Eq. (3.10).

It is interesting to also compare Eq. (3.10) to the inclusive measurements of the branching ratio in the high- q^2 region through the sum-over-exclusive approach at Belle [63, 64] and BaBar [65, 66], for $q^2 > 14.4 \text{ GeV}^2$ and $q^2 > 14.2 \text{ GeV}^2$, respectively. Due to the different cuts and the different treatment of the QED effects, the B factory measurements cannot be directly compared to the result of Eq. (3.10). In order to compare, we use the theoretical predictions for the different cuts and QED treatments to obtain a rescaling factor as discussed in more detail in the next section. We find

$$\mathcal{B}[> 15]_{\text{BaBar/Belle}} = (4.63 \pm 0.97) \times 10^{-7}. \quad (3.11)$$

In Fig. 1, we compare these two determinations with our theoretical predictions. On the experimental side, we see a slight tension between the BaBar/Belle and LHCb+ChiPT determinations. The slight tension between measurements of LHCb and the B factories is already visible on the level of exclusive modes [67, 68]: It is interesting to consider the sum-over-exclusives at the B factories in analogy to Eq. (3.10) and compare that to their respective inclusive determinations. As a rough estimate, we calculated the S -wave $K\pi$ contribution following [27] using a lower phase space cutoff of $q_0^2 = 14.2 \text{ GeV}^2$.⁸ Adding Belle and BaBar measurements of the exclusive rates, we find compatibility with the B factory average in Eq. (3.11).

Recently, the authors of Ref. [41] claimed that the tensions in the exclusive $b \rightarrow s\ell\ell$ modes at low- q^2 are independently verified in the semi-inclusive modes at high- q^2 , albeit with lower significance. It is evident that the full picture given by the four determinations in Fig. 1 does not show any tension with the SM.

This finding is further illustrated in the next subsection where we compare the different determinations at a common lower cutoff $q_0^2 = 14.4 \text{ GeV}^2$.

⁷We reproduce this number using the implementation of [27] with new inputs given in [41].

⁸One may be critical that the soft pion approximation in ChiPT applies for phase spaces as large as $q^2 > 14.2 \text{ GeV}^2$ though.

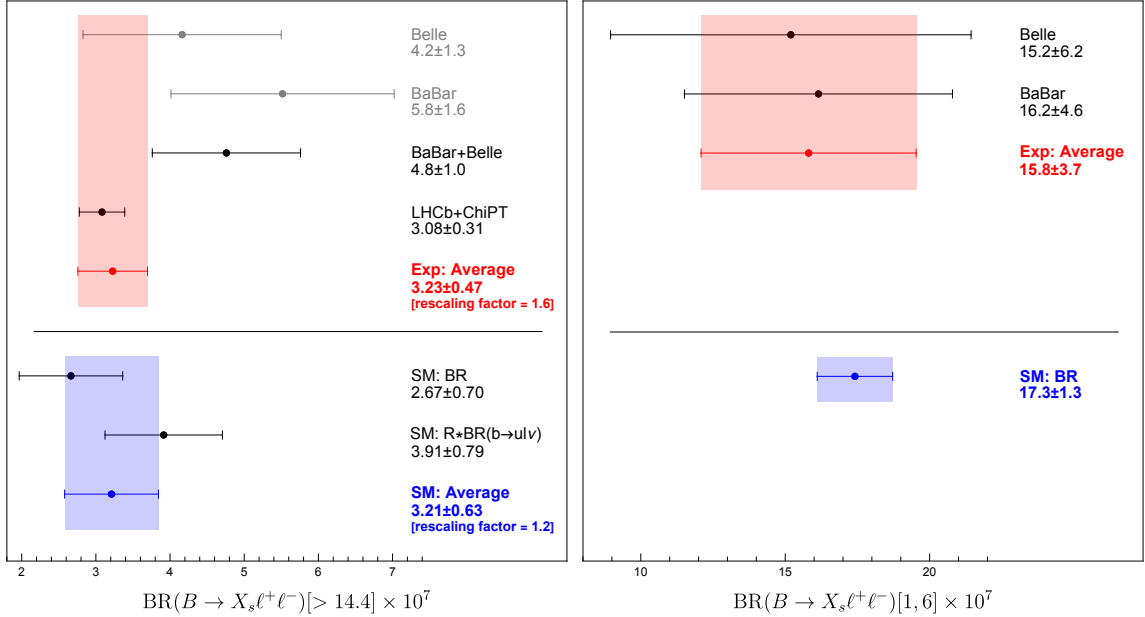


Figure 2: Measurements (red) and SM predictions (blue) for the $\bar{B} \rightarrow X_s \ell^+ \ell^-$ branching ratios in the low- q^2 (right) and high- q^2 (left) region. Left panel: all results have been adjusted to a common lower endpoint $q_0^2 = 14.4 \text{ GeV}^2$ and all results include the logarithmically enhanced QED corrections as described in the text.

3.3 Averaging experimental and theoretical results

In this section, we make a more sophisticated comparison between theory and experiment in the low- q^2 and the $q^2 > 14.4 \text{ GeV}^2$ regions. It is reasonable to consider a lower cutoff of $q_0^2 = 14.4 \text{ GeV}^2$, corresponding to a larger hadronic phase space for which the HQE is expected to be under better control.

The weighted average from BaBar [65, 66] and Belle [63, 64] in the low- q^2 region is

$$\mathcal{B}[1, 6]_{\text{exp average}} = (1.58 \pm 0.37) \times 10^{-6}. \quad (3.12)$$

Here also the average over electron and muon modes is taken. At low- q^2 no equivalent of the sum-over-exclusive measurements in (3.10) is available from LHCb. For the theoretical prediction, we update our determinations given in Ref. [9], with the updated inputs given in section 2. As discussed in the introduction and in more detail in Ref. [9], it is necessary to include the logarithmically enhanced QED corrections for the B-factory setup. We give our updated phenomenological results in Appendix A. These results are also summarized in the right panel of Fig. 2, showing excellent agreement between the theoretical predictions and the experimental measurements.

At high- q^2 , we are dealing with determinations at different cuts and with different setups that do or do not require the inclusion of QED effects. In Fig. 2, we compare all the available measurements rescaled to a common lower endpoint of $q_0^2 = 14.4 \text{ GeV}^2$ and including logarithmically enhanced QED effects. We also average the electron and muon

final states. The rescaling is done using the theoretical expressions for the branching ratios presented in Table 1 and Table 2. In a first step we convert the BaBar measurement from $q^2 > 14.2 \text{ GeV}^2$ (as presented in Ref. [66]) to $q^2 > 14.4 \text{ GeV}^2$; the corresponding conversion factor is 0.958. This way we obtain the effective BaBar measurement quoted in the left panel of Figure 2. We then proceed to average the BaBar and Belle measurements, which now correspond to the same phase space cuts, leading to

$$\mathcal{B}[> 14.4]_{\text{Belle/BaBar}} = (4.8 \pm 1.0) \times 10^{-7}. \quad (3.13)$$

In the previous subsection, we have rescaled this average to match a cut of 15 GeV^2 without QED effects. Taking the theoretical values from Table 1 and Table 2, we find the corresponding rescaling factor

$$\epsilon \equiv \frac{\mathcal{B}[> 15]_{\text{no QED}}}{\mathcal{B}[> 14.4]_{\text{with QED}}} = 0.97, \quad (3.14)$$

which is marginal due to a partial cancellation of phase space enhancement and QED bin migration. Multiplying the averaged branching ratio in Eq. (3.13) with this factor one finds the result given in Eq. (3.11).

In order to compare all results with the same cut $q_0^2 = 14.4 \text{ GeV}^2$ (as done in Fig. 2), we also need to rescale the determination of this branching ratio obtained from exclusive $B \rightarrow (K, K^*)\mu^+\mu^-$ measurement at LHCb for $q^2 > 15 \text{ GeV}^2$. Rescaling the original branching fraction given in Eq. (3.10) with the factor given in Eq. (3.14), we obtain

$$\mathcal{B}[> 14.4]_{\text{LHCb+ChiPT}} = (3.08 \pm 0.31) \times 10^{-7}. \quad (3.15)$$

Now we are in the position to average the BaBar/Belle determination from (3.13) and the LHCb+ChiPT one from (3.15) and find

$$\mathcal{B}[> 14.4]_{\text{exp average}} = (3.23 \pm 0.47) \times 10^{-7}. \quad (3.16)$$

The uncertainty of the weighted average in (3.16) has been inflated by a rescaling factor of 1.6. The latter has been obtained following the standard PDG procedure [69] and is equal to the square root of the reduced chi-square (i.e. divided by $N - 1$ when averaging N measurements) of the input measurements evaluated with respect to the weighted-average central value (see section 5.2.2 of Ref. [69]).

Note that we first average the BaBar and Belle measurements and then combine the latter with the LHCb+ChiPT determination. Alternatively it is possible to combine the three measurements directly (with $N = 3$) and obtain $\mathcal{B}[> 14.4] = (3.23 \pm 0.36) \times 10^{-7}$. The smaller uncertainty is due to the smaller rescaling factor, 1.2 versus 1.6, obtained while combining the three measurements simultaneously. We prefer the former averaging procedure because it is overall a more conservative approach and it also shows a clear comparison between two very different determinations of the branching ratio, namely the one measured by an e^+e^- experiment versus the one measured by a pp experiment supplemented by a ChiPT estimate of missing non-resonant modes.

We compare the result given in Eq. (3.16) to our theoretical predictions in Table 2. Averaging the direct branching ratio calculation with that obtained from the ratio \mathcal{R} , we find

$$\mathcal{B}[> 14.4]_{\text{SM average}} = (3.21 \pm 0.63) \times 10^{-7}, \quad (3.17)$$

which includes an error rescaling factor of 1.2 and implements the +0.20 theory correlation coefficient between $\mathcal{B}[> 14.4]$ and $\mathcal{R}(14.4)$ derived from the dependences on parametric inputs listed in Eqs. (3.2) and (3.3). Figure 2 shows a consistent picture of the average of the theory and the average of the experimental determinations.

4 New physics sensitivities

The sensitivity of $\bar{B} \rightarrow X_s \ell^+ \ell^-$ to physics beyond the Standard Model has improved in several respects since our previous analysis [9]. The high- q^2 branching ratio in Eq. (3.16) now incorporates LHCb measurements of exclusive $B \rightarrow K^{(*)}$ modes and is more precise than the Belle/BaBar average in Eq. (3.13). In addition, an analysis of the $\bar{B} \rightarrow X_u \ell \bar{\nu}$ distribution using the full Belle data set [57] has enabled a competitive phenomenological approach to the high- q^2 region through the ratio \mathcal{R} defined in Eq. (1.1).

Since $B \rightarrow K^{(*)} \ell^+ \ell^-$ decay rates into muons relative to electrons [70, 71] are consistent with predictions near unity [11], we constrain lepton flavor universal coefficients $C_{9,10} = C_{9,10}^\mu = C_{9,10}^e$, parameterized by new physics corrections $C_{9,10}^{\text{NP}} = C_{9,10} - C_{9,10}^{\text{SM}}$ ⁹.

To determine the current bounds, only the inclusive $\mathcal{B}[1, 6]$, $\mathcal{B}[> 14.4]$, $\mathcal{R}(14.4)$ and leptonic $\mathcal{B}(B_s \rightarrow \mu\mu)$ constraints are considered. For the experimental inputs, we use the inclusive branching ratios in Eqs. (3.12), (3.16) and (3.5), and the average

$$\mathcal{B}(B_s \rightarrow \mu\mu)_{\text{exp average}} = (3.45 \pm 0.29) \times 10^{-9} \quad (4.1)$$

of the measurements of the leptonic mode [72–76] from HFLAV [77]. For the theory, we generated predictions for general $C_{9,10}^{\text{NP}}$ which are consistent with the central values of $\mathcal{B}[1, 6]$, $\mathcal{B}[> 14.4]$ and $\mathcal{R}(14.4)$ given in Table 2 at the Standard Model point ($C_{9,10}^{\text{NP}} = 0$). Uncertainties of inclusive observables were assumed to scale with their central values in the $C_{9,10}^{\text{NP}}$ plane. The central value and uncertainty of $\mathcal{B}(B_s \rightarrow \mu\mu)$ as functions of $C_{9,10}^{\text{NP}}$ were obtained in Flavio [78], consistent with

$$\mathcal{B}(B_s \rightarrow \mu\mu)_{\text{SM}} = (3.66 \pm 0.14) \times 10^{-9} \quad (4.2)$$

from Ref. [79] at the point $C_{9,10}^{\text{NP}} = 0$.

Although $\mathcal{R}(14.4)$ is preferred compared to the branching ratio $\mathcal{B}[> 14.4]$ on theoretical grounds, due to the experimental uncertainty on $\bar{B} \rightarrow X_u \ell \bar{\nu}$, the constraint from the direct determination $\mathcal{B}[> 14.4]$ is competitive to the indirect determination. The current constraints on C_9^{NP} and C_{10}^{NP} are shown in Figure 3, with (left panel) and without (right panel) using $\bar{B} \rightarrow X_u \ell \bar{\nu}$ inputs at high- q^2 . In either approach, both the high- q^2 and the combined constraints are consistent with the Standard Model. The same fits in the

⁹Coefficients are renormalized at the electroweak scale $\mu_0 = 120 \text{ GeV}$ in the $\overline{\text{MS}}$ scheme.

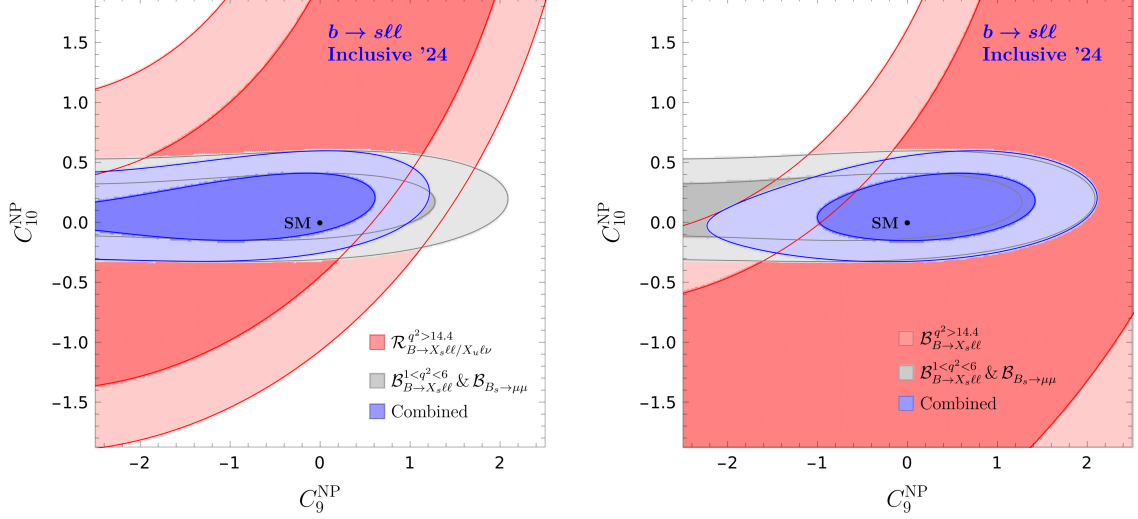


Figure 3: Constraints on $b \rightarrow s\ell\ell$ coefficients from inclusive and leptonic modes, with (left panel) and without (right panel) normalizing $\mathcal{B}(\bar{B} \rightarrow X_s \ell^+ \ell^-)$ to $\mathcal{B}(\bar{B} \rightarrow X_u \ell \bar{\nu})$ in the high- q^2 region. Light and dark bands correspond to 68% and 95% confidence intervals.

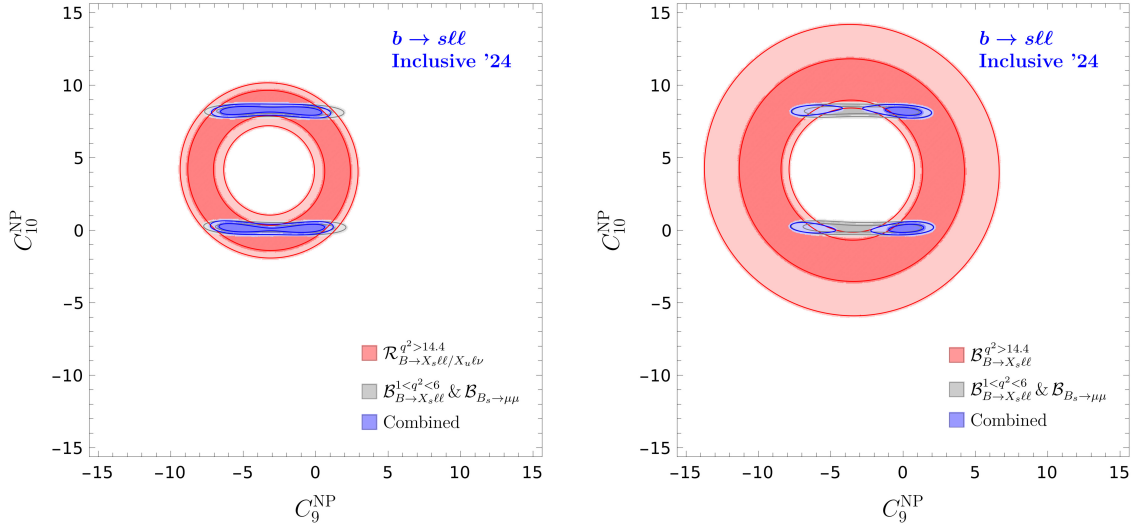


Figure 4: Constraints on $b \rightarrow s\ell\ell$ coefficients from inclusive and leptonic modes in the expanded plane. See Figure 3 for further details.

expanded plane are shown in Figure 4. The constraint from $\mathcal{B}[\geq 14.4]$ relaxes for unrealistically large new physics deviations since the theory uncertainty is large compared to $\mathcal{R}(14.4)$ and scales with the central value, which becomes large at the boundaries of the panel.

The decomposition of the inclusive rate into three angular observables will play a crucial role in future precision analyses of $\bar{B} \rightarrow X_s \ell^+ \ell^-$ at Belle II. For the corresponding projection, we adopt the experimental uncertainties for the angular observables in Table 4

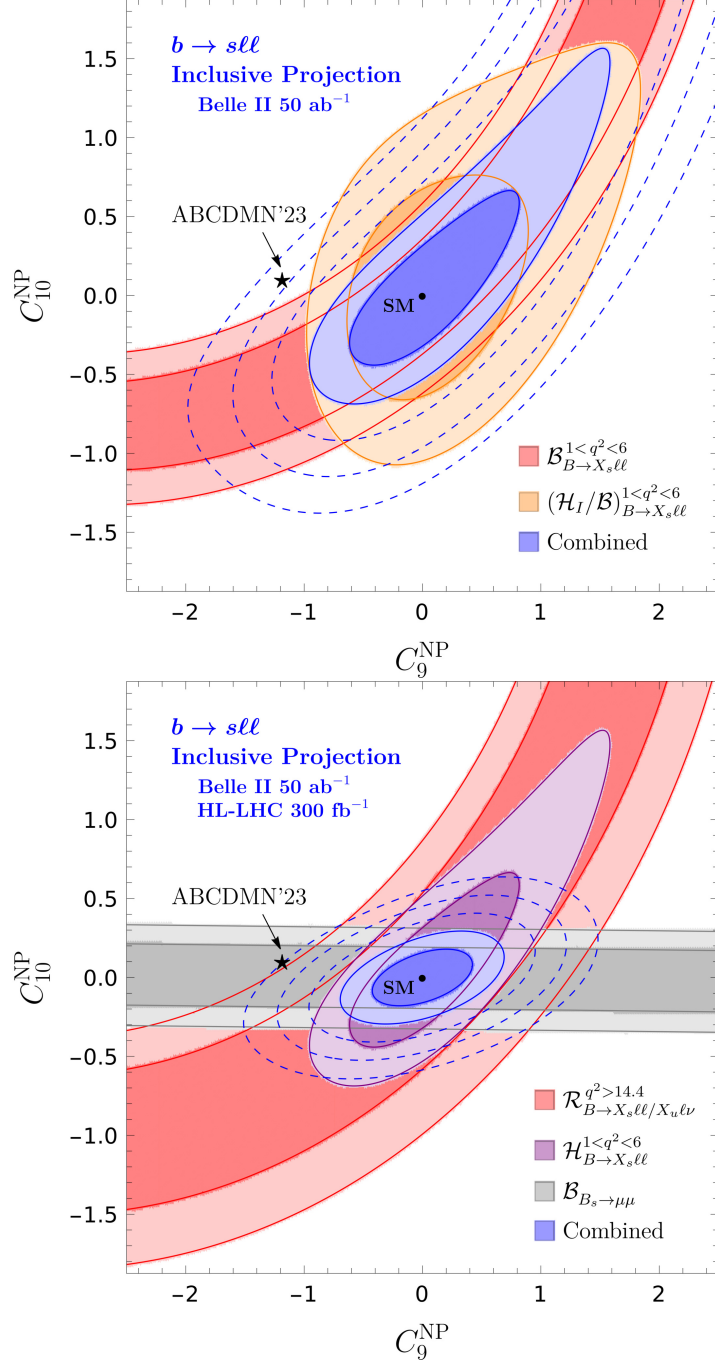


Figure 5: Projected constraints on $b \rightarrow sll$ coefficients centered on the Standard Model. In the lower panel high- q^2 projections at Belle II are combined with the $B_s \rightarrow \mu\mu$ projection at the HL-LHC. Light and dark bands of each colour correspond to 68% and 95% confidence intervals; radiating dashed lines are the 3σ , 4σ and 5σ contours, respectively. The central value of a fit including exclusive semileptonic modes [80] is shown by an asterisk for comparison. See text for further explanations.

of Ref. [9] corresponding to 50 ab^{-1} integrated luminosity [81], and assume measurements centered on the predictions in Table 2. In the upper panel of Figure 5, we compare the projected combined constraint in this region (blue) to the constraints from the rate (red) and angular observables (yellow). We note that in the $C_{10}^{\text{NP}} = 0$ scenario, the combined constraint on C_9^{NP} is significantly stronger than the constraints from the rate and angular observables separately. The angular constraint is a combination of four constraints from two independent normalized angular observables chosen as $\mathcal{H}_T/\mathcal{B}$ and $\mathcal{H}_A/\mathcal{B}$ separated into two bins $1 \text{ GeV}^2 < q^2 < 3.5 \text{ GeV}^2$ and $3.5 \text{ GeV}^2 < q^2 < 6 \text{ GeV}^2$. The intersection of the two hyperbolic constraints from \mathcal{H}_A and two circular constraints from \mathcal{H}_T (see Fig. 3 of [9]) generates the elongated elliptical shape of the yellow band in Figure 5 (distorted slightly by the normalization to the rate). The normalization is conceptually important, as it suppresses the nonperturbative effect of the hadronic mass cut in the low- q^2 region [40].

In the high- q^2 region, from the current precision in Eq. (3.7) improved by a factor of 3.5 (the expected improvement in inclusive $|V_{ub}|$ determination at Belle II [81]), we project $\delta\mathcal{B}(\bar{B} \rightarrow X_u \ell \bar{\nu})[> 14.4] = 5.2\%$. Combined with $\delta\mathcal{B}(\bar{B} \rightarrow X_s \ell^+ \ell^-)[> 14.4] = 4.7\%$ in quadrature, one obtains $\delta\mathcal{R}(14.4) = 7.0\%$.¹⁰ It will be interesting to see whether future determinations of power correction parameters will enable a competitive constraint from $\mathcal{B}[> 14.4]$, which is not included in the projection. For the leptonic mode we take $\delta\mathcal{B}(B_s \rightarrow \mu\mu) = 4.8\%$ corresponding to 300 fb^{-1} at the HL-LHC [82].

Including the projected constraints from \mathcal{R} and $B_s \rightarrow \mu\mu$ (lower panel of Figure 5) contracts the 5σ contour near the central value of a fit including exclusive semileptonic modes [80]. This panel highlights the role of the inclusive mode in scrutinizing whether new short-distance physics is responsible for the anomaly in the exclusive modes. Inclusive measurements with 50 ab^{-1} consistent with the Standard Model would exclude the $C_9^{\text{NP}} \simeq -1$ scenario. However, anomalous inclusive measurements favoring negative C_9^{NP} would provide compelling evidence in favor of the new physics interpretation of the exclusive anomalies. The current constraints in Fig. 3 are inconclusive, as they are consistent with the Standard Model as well as scenarios with large negative C_9^{NP} .

Finally, the promising situation at Belle II would benefit from a novel semi-inclusive measurement of $\bar{B} \rightarrow X_s \ell^+ \ell^-$ at LHCb [5]. At least in the high- q^2 region, the inclusive mode can be reliably extrapolated from the sum of several exclusive modes, and updated measurements of the exclusive modes can be expected from LHC experiments in the near future. For instance, an analysis of $B^+ \rightarrow K^+ \ell^+ \ell^-$ at CMS has recently become available [83].

5 Conclusion

Motivated by a proposed semi-inclusive analysis at LHCb [5], we have presented predictions for inclusive $\bar{B} \rightarrow X_s \ell^+ \ell^-$ observables suitable to the hadron collider environment. Due to the limited hadronic phase space in the high- q^2 region, the inclusive rate can already be extrapolated from K and K^* modes at LHCb [41]. It is likely that a semi-inclusive

¹⁰This marginally updates our projection $\delta\mathcal{R}(14.4) = 7.3\%$ in Ref. [9].

analysis will require simulation of collinear photon radiation, as was the case for exclusive measurements at LHCb, but not at the B factories. To confront the various experimental determinations to each other and to the Standard Model, we have investigated the effect of including collinear photon radiation in our computations, as well as the dependence of the endpoint q_0^2 in the high- q^2 region $q^2 > q_0^2$. In the low- q^2 region we also calculate the branching ratio and three angular observables separated into two bins.

The inclusive rate in the high- q^2 region is very sensitive to power corrections of order $1/m_b^2$, $1/m_b^3$ and $1/m_c^2$. To reduce the sensitivity to the $1/m_b$ corrections, we calculate the ratio \mathcal{R} of the $\bar{B} \rightarrow X_s \ell^+ \ell^-$ and $\bar{B} \rightarrow X_u \ell \bar{\nu}$ branching ratios with the same phase space cut [29]. Multiplying this ratio by the experimental $\bar{B} \rightarrow X_u \ell \bar{\nu}$ branching ratio results in an indirect determination of the high- q^2 branching ratio competitive with the direct theoretical determination, with uncertainty dominated by experimental input rather than power correction parameters. We find that the consistency improves as the endpoint is lowered from $q_0^2 = 15 \text{ GeV}^2$ to $q_0^2 = 14.4 \text{ GeV}^2$, which increases the hadronic phase space, as expected. It will be interesting to see whether the direct and indirect determinations continue to converge with more statistics on the charged current process and more precise determinations of power correction parameters.

We find compatibility between our theoretical determinations of the inclusive rate at high- q^2 and our extrapolation of the sum over $B \rightarrow K$ and $B \rightarrow K^*$ modes from LHCb to the inclusive rate adapted from Ref. [41]. After correcting for phase space and collinear photon radiation, the average of LHCb and B-factory results significantly improves the sensitivity of the inclusive mode to physics beyond the Standard Model. The resulting constraint from the inclusive and $B_s \rightarrow \mu\mu$ modes is consistent with the Standard Model, but new physics corrections to the vector coefficient C_9 as large as the Standard Model contribution cannot be excluded yet. We emphasize that the theory uncertainties dominate at high- q^2 , but in fact originate from sources which are essentially driven by experiment (in particular, $\bar{B} \rightarrow X_u \ell \bar{\nu}$).

In the future, an experimental determination of the sum of K and $K\pi$ modes at high- q^2 (without resolving the $K\pi$ subsystem, i.e. the K^* lineshape) would limit the theory input needed to extrapolate to the inclusive mode. A semi-inclusive measurement at low- q^2 is much more complicated due to the multiplicity of states including neutral pions.

The projected sensitivity to physics beyond the Standard Model with 50 ab^{-1} at Belle II is already quite promising; inclusive measurements consistent with the Standard Model would exclude the $C_9^{\text{NP}} \simeq -1$ scenario at high confidence. This projection would benefit from a semi-inclusive measurement of $\bar{B} \rightarrow X_s \ell^+ \ell^-$ at the LHC [5].

Acknowledgements

We thank Patrick Owen, Ulrik Egede and Johannes Albrecht for discussions on the treatment of photons in LHCb. In addition, we thank Florian Bernlochner and Lu Cao for extensive discussions on the treatment of photons in Belle II. We also thank M eril Reboud for discussions on statistical analyses.

The work of QQ was supported in part by the National Natural Science Foundation of China under Grant No. 12375086. The work of EL was supported in part by the U.S.

$$\bar{B} \rightarrow X_s \ell^+ \ell^- \quad (\ell = e, \mu \text{ average})$$

q^2 range [GeV ²]	[1, 6]	[1, 3.5]	[3.5, 6]
\mathcal{B} [10 ⁻⁷]	17.41 ± 1.31	9.58 ± 0.65	7.83 ± 0.67
\mathcal{H}_T [10 ⁻⁷]	4.77 ± 0.40	2.50 ± 0.18	2.27 ± 0.22
\mathcal{H}_L [10 ⁻⁷]	12.65 ± 0.92	7.085 ± 0.48	5.56 ± 0.45
\mathcal{H}_A [10 ⁻⁷]	-0.10 ± 0.21	-0.989 ± 0.080	0.89 ± 0.16
q^2 range [GeV ²]	> 14.4		
\mathcal{B} [10 ⁻⁷]	2.66 ± 0.70		
$\mathcal{R}(q_0^2)$ [10 ⁻⁴]	24.12 ± 2.01		

Table 2: Phenomenological results including log-enhanced QED corrections to the $\bar{B} \rightarrow X_s \ell^+ \ell^-$ process. All quantities are obtained by averaging $\ell = e, \mu$. The denominator of the ratio $\mathcal{R}(q_0^2)$ (i.e. the $\bar{B} \rightarrow X_u \ell \bar{\nu}$ rate for $q^2 > q_0^2$), on the other hand, does not include effects which correspond to log-enhanced QED corrections on the theory side. See text for further details.

Department of Energy under grant number DE-SC0010120. The work of T. Huber and JJ was supported in part by the Deutsche Forschungsgemeinschaft (DFG, German Research Foundation) under grant 396021762 - TRR 257 “Particle Physics Phenomenology after the Higgs Discovery”. The work of T. Hurth was supported by the Cluster of Excellence ‘Precision Physics, Fundamental Interactions, and Structure of Matter’ (PRISMA+ EXC 2118/1) funded by the German Research Foundation (DFG) within the German Excellence Strategy (Project ID 390831469). He also thanks the CERN theory group for its hospitality during his regular visits to CERN where part of this work was written. KKV acknowledges support from the Dutch Research Council (NWO) in the form of the VIDI grant “Solving Beautiful Puzzles”.

A Standard Model predictions for the B factories

In this section, we present updated predictions for several observables including the logarithmically enhanced QED corrections as in [7–9]. We stress again that these predictions are suitable for fully inclusive measurements at the B factories. We update these predictions, which we used in section 3.3, in Table 2, in particular due to changes in HQE input parameters for the high- q^2 observables. Due to the QED effects, one has to distinguish between the muon and electron final states. Here we average both as is done in the current experimental measurements.

In addition, the prediction for the ratio \mathcal{R} does not include QED effects for the $b \rightarrow u$ transition. This is because we later multiply the measured quantity by (3.5) in which these effects should not be taken into account¹¹.

¹¹We thank Florian Bernlochner and Lu Cao for discussion about the $b \rightarrow u$ measurement.

References

- [1] A. Greljo, J. Salko, A. Smolkovič and P. Stangl, *Rare b decays meet high-mass Drell-Yan*, *JHEP* **05** (2023) 087 [[2212.10497](#)].
- [2] M. Ciuchini, M. Fedele, E. Franco, A. Paul, L. Silvestrini and M. Valli, *Constraints on lepton universality violation from rare B decays*, *Phys. Rev. D* **107** (2023) 055036 [[2212.10516](#)].
- [3] M. Algueró, A. Biswas, B. Capdevila, S. Descotes-Genon, J. Matias and M. Novoa-Brunet, *To $(b)e$ or not to $(b)e$: no electrons at LHCb*, *Eur. Phys. J. C* **83** (2023) 648 [[2304.07330](#)].
- [4] T. Hurth, F. Mahmoudi and S. Neshatpour, *B anomalies in the post $R_{K^{(*)}}$ era*, [2310.05585](#).
- [5] Y. Amhis and P. Owen, *Isospin extrapolation as a method to study inclusive $\bar{B} \rightarrow X_s \ell^+ \ell^-$ decays*, *Eur. Phys. J. C* **82** (2022) 371 [[2106.15943](#)].
- [6] T. Huber, E. Lunghi, M. Misiak and D. Wyler, *Electromagnetic logarithms in $\bar{B} \rightarrow X_s l^+ l^-$* , *Nucl. Phys. B* **740** (2006) 105 [[hep-ph/0512066](#)].
- [7] T. Huber, T. Hurth and E. Lunghi, *Logarithmically Enhanced Corrections to the Decay Rate and Forward Backward Asymmetry in $\bar{B} \rightarrow X_s \ell^+ \ell^-$* , *Nucl. Phys. B* **802** (2008) 40 [[0712.3009](#)].
- [8] T. Huber, T. Hurth and E. Lunghi, *Inclusive $\bar{B} \rightarrow X_s \ell^+ \ell^-$: complete angular analysis and a thorough study of collinear photons*, *JHEP* **06** (2015) 176 [[1503.04849](#)].
- [9] T. Huber, T. Hurth, J. Jenkins, E. Lunghi, Q. Qin and K. K. Vos, *Phenomenology of inclusive $\bar{B} \rightarrow X_s \ell^+ \ell^-$ for the Belle II era*, *JHEP* **10** (2020) 088 [[2007.04191](#)].
- [10] D. Bigi, M. Bordone, P. Gambino, U. Haisch and A. Piccione, *QED effects in inclusive semi-leptonic B decays*, *JHEP* **11** (2023) 163 [[2309.02849](#)].
- [11] M. Bordone, G. Isidori and A. Pattori, *On the Standard Model predictions for R_K and R_{K^*}* , *Eur. Phys. J. C* **76** (2016) 440 [[1605.07633](#)].
- [12] G. Isidori, D. Lancerini, S. Nabeebaccus and R. Zwicky, *QED in $\bar{B} \rightarrow \bar{K} \ell^+ \ell^-$ LFU ratios: theory versus experiment, a Monte Carlo study*, *JHEP* **10** (2022) 146 [[2205.08635](#)].
- [13] G. Isidori, S. Nabeebaccus and R. Zwicky, *QED corrections in $\bar{B} \rightarrow \bar{K} \ell^+ \ell^-$ at the double-differential level*, *JHEP* **12** (2020) 104 [[2009.00929](#)].
- [14] C. Bobeth, M. Misiak and J. Urban, *Photonic penguins at two loops and m_t dependence of $BR[B \rightarrow X_s l^+ l^-]$* , *Nucl. Phys. B* **574** (2000) 291 [[hep-ph/9910220](#)].
- [15] H. H. Asatryan, H. M. Asatrian, C. Greub and M. Walker, *Calculation of two loop virtual corrections to $b \rightarrow sl^+ l^-$ in the standard model*, *Phys. Rev. D* **65** (2002) 074004 [[hep-ph/0109140](#)].
- [16] H. H. Asatrian, H. M. Asatrian, C. Greub and M. Walker, *Two loop virtual corrections to $B \rightarrow X_s l^+ l^-$ in the standard model*, *Phys. Lett. B* **507** (2001) 162 [[hep-ph/0103087](#)].
- [17] H. H. Asatryan, H. M. Asatrian, C. Greub and M. Walker, *Complete gluon bremsstrahlung corrections to the process $b \rightarrow sl^+ l^-$* , *Phys. Rev. D* **66** (2002) 034009 [[hep-ph/0204341](#)].
- [18] A. Ghinculov, T. Hurth, G. Isidori and Y. P. Yao, *Forward backward asymmetry in $B \rightarrow X_s l^+ l^-$ at the NNLL level*, *Nucl. Phys. B* **648** (2003) 254 [[hep-ph/0208088](#)].
- [19] H. M. Asatrian, K. Bieri, C. Greub and A. Hovhannisyan, *NNLL corrections to the angular distribution and to the forward backward asymmetries in $B \rightarrow X_s l^+ l^-$* , *Phys. Rev. D* **66** (2002) 094013 [[hep-ph/0209006](#)].

- [20] A. Ghinculov, T. Hurth, G. Isidori and Y. P. Yao, *The Rare decay $B \rightarrow X_s l^+ l^-$ to NNLL precision for arbitrary dilepton invariant mass*, *Nucl. Phys. B* **685** (2004) 351 [[hep-ph/0312128](#)].
- [21] C. Greub, V. Pilipp and C. Schubach, *Analytic calculation of two-loop QCD corrections to $b \rightarrow sl^+ l^-$ in the high q^2 region*, *JHEP* **12** (2008) 040 [[0810.4077](#)].
- [22] S. de Boer, *Two loop virtual corrections to $b \rightarrow (d, s) \ell^+ \ell^-$ and $c \rightarrow u \ell^+ \ell^-$ for arbitrary momentum transfer*, *Eur. Phys. J. C* **77** (2017) 801 [[1707.00988](#)].
- [23] C. Bobeth, P. Gambino, M. Gorbahn and U. Haisch, *Complete NNLO QCD analysis of anti- $B \rightarrow X(s) l^+ l^-$ and higher order electroweak effects*, *JHEP* **04** (2004) 071 [[hep-ph/0312090](#)].
- [24] A. F. Falk, M. E. Luke and M. J. Savage, *Nonperturbative contributions to the inclusive rare decays $B \rightarrow X_s \gamma$ and $B \rightarrow X_s l^+ l^-$* , *Phys. Rev. D* **49** (1994) 3367 [[hep-ph/9308288](#)].
- [25] A. Ali, G. Hiller, L. T. Handoko and T. Morozumi, *Power corrections in the decay rate and distributions in $B \rightarrow X_s l^+ l^-$ in the Standard Model*, *Phys. Rev. D* **55** (1997) 4105 [[hep-ph/9609449](#)].
- [26] J.-W. Chen, G. Rupak and M. J. Savage, *Non- $1/m_b^n$ power suppressed contributions to inclusive $B \rightarrow X_s l^+ l^-$ decays*, *Phys. Lett. B* **410** (1997) 285 [[hep-ph/9705219](#)].
- [27] G. Buchalla and G. Isidori, *Nonperturbative effects in $\bar{B} \rightarrow X_s l^+ l^-$ for large dilepton invariant mass*, *Nucl. Phys. B* **525** (1998) 333 [[hep-ph/9801456](#)].
- [28] C. W. Bauer and C. N. Burrell, *Nonperturbative corrections to moments of the decay $B \rightarrow X_s \ell^+ \ell^-$* , *Phys. Rev. D* **62** (2000) 114028 [[hep-ph/9911404](#)].
- [29] Z. Ligeti and F. J. Tackmann, *Precise predictions for $B \rightarrow X_s l^+ l^-$ in the large q^2 region*, *Phys. Lett. B* **653** (2007) 404 [[0707.1694](#)].
- [30] T. Huber, Q. Qin and K. K. Vos, *Five-particle contributions to the inclusive rare $\bar{B} \rightarrow X_{s(d)} \ell^+ \ell^-$ decays*, *Eur. Phys. J. C* **78** (2018) 748 [[1806.11521](#)].
- [31] F. Kruger and L. M. Sehgal, *Lepton polarization in the decays $b \rightarrow X_{(s)} \mu^+ \mu^-$ and $B \rightarrow X_{(s)} \tau^+ \tau^-$* , *Phys. Lett. B* **380** (1996) 199 [[hep-ph/9603237](#)].
- [32] F. Kruger and L. M. Sehgal, *CP violation in the decay $B \rightarrow X_{(d)} e^+ e^-$* , *Phys. Rev. D* **55** (1997) 2799 [[hep-ph/9608361](#)].
- [33] G. Buchalla, G. Isidori and S. J. Rey, *Corrections of order Λ_{QCD}^2/m_c^2 to inclusive rare B decays*, *Nucl. Phys. B* **511** (1998) 594 [[hep-ph/9705253](#)].
- [34] T. Huber, T. Hurth, J. Jenkins, E. Lunghi, Q. Qin and K. K. Vos, *Long distance effects in inclusive rare B decays and phenomenology of $\bar{B} \rightarrow X_d \ell^+ \ell^-$* , *JHEP* **10** (2019) 228 [[1908.07507](#)].
- [35] M. Benzke, T. Hurth and S. Turczyk, *Subleading power factorization in $\bar{B} \rightarrow X_s \ell^+ \ell^-$* , *JHEP* **10** (2017) 031 [[1705.10366](#)].
- [36] T. Hurth, M. Fickinger, S. Turczyk and M. Benzke, *Resolved Power Corrections to the Inclusive Decay $\bar{B} \rightarrow X_s \ell^+ \ell^-$* , *Nucl. Part. Phys. Proc.* **285-286** (2017) 57 [[1711.01162](#)].
- [37] M. Benzke and T. Hurth, *Resolved $1/m_b$ contributions to $\bar{B} \rightarrow X_{s,d} \ell^+ \ell^-$ and $\bar{B} \rightarrow X_s \gamma$* , *Phys. Rev. D* **102** (2020) 114024 [[2006.00624](#)].
- [38] K. S. M. Lee, Z. Ligeti, I. W. Stewart and F. J. Tackmann, *Universality and m_X cut effects in $B \rightarrow X_s l^+ l^-$* , *Phys. Rev. D* **74** (2006) 011501 [[hep-ph/0512191](#)].

- [39] K. S. M. Lee and F. J. Tackmann, *Nonperturbative m_X cut effects in $B \rightarrow X_s l^+ l^-$ observables*, *Phys. Rev. D* **79** (2009) 114021 [[0812.0001](#)].
- [40] T. Huber, T. Hurth, J. Jenkins and E. Lunghi, *Inclusive $\bar{B} \rightarrow X_s \ell^+ \ell^-$ with a hadronic mass cut*, *JHEP* **12** (2023) 117 [[2306.03134](#)].
- [41] G. Isidori, Z. Polonsky and A. Tinari, *Semi-inclusive $b \rightarrow s \ell \ell$ transitions at high q^2* , *Phys. Rev. D* **108** (2023) 093008 [[2305.03076](#)].
- [42] M. B. Voloshin, *Nonfactorization effects in heavy mesons and determination of $-V(ub)-$ from inclusive semileptonic B decays*, *Phys. Lett. B* **515** (2001) 74 [[hep-ph/0106040](#)].
- [43] P. Gambino and J. F. Kamenik, *Lepton energy moments in semileptonic charm decays*, *Nucl. Phys. B* **840** (2010) 424 [[1004.0114](#)].
- [44] M. Bordone, B. Capdevila and P. Gambino, *Three loop calculations and inclusive V_{cb}* , *Phys. Lett. B* **822** (2021) 136679 [[2107.00604](#)].
- [45] F. Bernlochner, M. Fael, K. Olschewsky, E. Persson, R. van Tonder, K. K. Vos et al., *First extraction of inclusive V_{cb} from q^2 moments*, *JHEP* **10** (2022) 068 [[2205.10274](#)].
- [46] M. Fael, T. Mannel and K. Keri Vos, *V_{cb} determination from inclusive $b \rightarrow c$ decays: an alternative method*, *JHEP* **02** (2019) 177 [[1812.07472](#)].
- [47] G. Finauri and P. Gambino, *The q^2 moments in inclusive semileptonic B decays*, [2310.20324](#).
- [48] I. I. Y. Bigi, M. A. Shifman, N. G. Uraltsev and A. I. Vainshtein, *Sum rules for heavy flavor transitions in the SV limit*, *Phys. Rev. D* **52** (1995) 196 [[hep-ph/9405410](#)].
- [49] I. I. Y. Bigi, M. A. Shifman, N. Uraltsev and A. I. Vainshtein, *High power n of $m(b)$ in beauty widths and $n = 5 \rightarrow$ infinity limit*, *Phys. Rev. D* **56** (1997) 4017 [[hep-ph/9704245](#)].
- [50] P. Gambino and N. Uraltsev, *Moments of semileptonic B decay distributions in the $1/m(b)$ expansion*, *Eur. Phys. J. C* **34** (2004) 181 [[hep-ph/0401063](#)].
- [51] A. Alberti, P. Gambino, K. J. Healey and S. Nandi, *Precision Determination of the Cabibbo-Kobayashi-Maskawa Element V_{cb}* , *Phys. Rev. Lett.* **114** (2015) 061802 [[1411.6560](#)].
- [52] M. Fael, K. Schönwald and M. Steinhauser, *Relation between the $\overline{\text{MS}}$ and the kinetic mass of heavy quarks*, *Phys. Rev. D* **103** (2021) 014005 [[2011.11655](#)].
- [53] L.-B. Chen, H. T. Li, Z. Li, J. Wang, Y. Wang and Q.-f. Wu, *Analytic three-loop QCD corrections to top-quark and semileptonic $b \rightarrow u$ decays*, [2309.00762](#).
- [54] M. Fael and J. Usovitsch, *Third order correction to semileptonic $b \rightarrow u$ decay: fermionic contributions*, [2310.03685](#).
- [55] M. Neubert, *On the inclusive determination of $-V(ub)-$ from the lepton invariant mass spectrum*, *JHEP* **07** (2000) 022 [[hep-ph/0006068](#)].
- [56] C. W. Bauer, Z. Ligeti and M. E. Luke, *Precision determination of $-V(ub)-$ from inclusive decays*, *Phys. Rev. D* **64** (2001) 113004 [[hep-ph/0107074](#)].
- [57] BELLE collaboration, *Measurement of Differential Branching Fractions of Inclusive $B \rightarrow X_u \ell^+ \nu_\ell$ Decays*, *Phys. Rev. Lett.* **127** (2021) 261801 [[2107.13855](#)].
- [58] H. M. Asatrian, C. Greub and J. Virto, *Exact NLO matching and analyticity in $b \rightarrow s \ell \ell$* , *JHEP* **04** (2020) 012 [[1912.09099](#)].

- [59] C. Bobeth, M. Gorbahn and E. Stamou, *Electroweak Corrections to $B_{s,d} \rightarrow \ell^+ \ell^-$* , *Phys. Rev. D* **89** (2014) 034023 [[1311.1348](#)].
- [60] G. Buchalla and A. J. Buras, *Two loop large m_t electroweak corrections to $K \rightarrow \pi \nu \bar{\nu}$ for arbitrary Higgs boson mass*, *Phys. Rev. D* **57** (1998) 216 [[hep-ph/9707243](#)].
- [61] LHCb collaboration, *Differential branching fractions and isospin asymmetries of $B \rightarrow K^{(*)} \mu^+ \mu^-$ decays*, *JHEP* **06** (2014) 133 [[1403.8044](#)].
- [62] LHCb collaboration, *Measurements of the S-wave fraction in $B^0 \rightarrow K^+ \pi^- \mu^+ \mu^-$ decays and the $B^0 \rightarrow K^{*0} \mu^+ \mu^-$ differential branching fraction*, *JHEP* **11** (2016) 047 [[1606.04731](#)].
- [63] BELLE collaboration, *Improved measurement of the electroweak penguin process $B \rightarrow X_s \ell^+ \ell^-$* , *Phys. Rev. D* **72** (2005) 092005 [[hep-ex/0503044](#)].
- [64] BELLE collaboration, *Measurement of the lepton forward-backward asymmetry in $B \rightarrow X_s \ell^+ \ell^-$ decays with a sum of exclusive modes*, *Phys. Rev. D* **93** (2016) 032008 [[1402.7134](#)].
- [65] BABAR collaboration, *Measurement of the $B \rightarrow X_s \ell^+ \ell^-$ branching fraction with a sum over exclusive modes*, *Phys. Rev. Lett.* **93** (2004) 081802 [[hep-ex/0404006](#)].
- [66] BABAR collaboration, *Measurement of the $B \rightarrow X_s \ell^+ \ell^-$ branching fraction and search for direct CP violation from a sum of exclusive final states*, *Phys. Rev. Lett.* **112** (2014) 211802 [[1312.5364](#)].
- [67] BELLE collaboration, *Measurement of the Differential Branching Fraction and Forward-Backward Asymmetry for $B \rightarrow K^{(*)} \ell^+ \ell^-$* , *Phys. Rev. Lett.* **103** (2009) 171801 [[0904.0770](#)].
- [68] BABAR collaboration, *Measurement of Branching Fractions and Rate Asymmetries in the Rare Decays $B \rightarrow K^{(*)} \ell^+ \ell^-$* , *Phys. Rev. D* **86** (2012) 032012 [[1204.3933](#)].
- [69] P. D. Group, R. L. Workman, V. D. Burkert, V. Crede, E. Klempt, U. Thoma et al., *Review of Particle Physics*, *Progress of Theoretical and Experimental Physics* **2022** (2022) 083C01 [<https://academic.oup.com/ptep/article-pdf/2022/8/083C01/49175539/ptac097.pdf>].
- [70] LHCb collaboration, *Measurement of lepton universality parameters in $B^+ \rightarrow K^+ \ell^+ \ell^-$ and $B^0 \rightarrow K^{*0} \ell^+ \ell^-$ decays*, *Phys. Rev. D* **108** (2023) 032002 [[2212.09153](#)].
- [71] LHCb collaboration, *Test of lepton universality in $b \rightarrow s \ell^+ \ell^-$ decays*, *Phys. Rev. Lett.* **131** (2023) 051803 [[2212.09152](#)].
- [72] ATLAS collaboration, *Study of the rare decays of B_s^0 and B^0 mesons into muon pairs using data collected during 2015 and 2016 with the ATLAS detector*, *JHEP* **04** (2019) 098 [[1812.03017](#)].
- [73] LHCb collaboration, *Measurement of the $B_s^0 \rightarrow \mu^+ \mu^-$ decay properties and search for the $B^0 \rightarrow \mu^+ \mu^-$ and $B_s^0 \rightarrow \mu^+ \mu^- \gamma$ decays*, *Phys. Rev. D* **105** (2022) 012010 [[2108.09283](#)].
- [74] LHCb collaboration, *Analysis of Neutral B-Meson Decays into Two Muons*, *Phys. Rev. Lett.* **128** (2022) 041801 [[2108.09284](#)].
- [75] CMS collaboration, *Measurement of the $B_S^0 \rightarrow \mu^+ \mu^-$ decay properties and search for the $B^0 \rightarrow \mu^+ \mu^-$ decay in proton-proton collisions at $\sqrt{s} = 13$ TeV*, *Phys. Lett. B* **842** (2023) 137955 [[2212.10311](#)].
- [76] CDF collaboration, *Search for $B_s^0 \rightarrow \mu^+ \mu^-$ and $B^0 \rightarrow \mu^+ \mu^-$ Decays with the Full CDF Run II Data Set*, *Phys. Rev. D* **87** (2013) 072003 [[1301.7048](#)].

- [77] HFLAV collaboration, *Averages of b -hadron, c -hadron, and τ -lepton properties as of 2021*, *Phys. Rev. D* **107** (2023) 052008 [[2206.07501](#)].
- [78] D. M. Straub, *flavio: a Python package for flavour and precision phenomenology in the Standard Model and beyond*, [1810.08132](#).
- [79] M. Beneke, C. Bobeth and R. Szafron, *Power-enhanced leading-logarithmic QED corrections to $B_q \rightarrow \mu^+ \mu^-$* , *JHEP* **10** (2019) 232 [[1908.07011](#)].
- [80] B. Capdevila, *Status of the global $b \rightarrow s \ell^+ \ell^-$ fits*, *PoS FPCP2023* (2023) 010.
- [81] BELLE-II collaboration, *The Belle II Physics Book*, *PTEP* **2019** (2019) 123C01 [[1808.10567](#)].
- [82] A. Cerri et al., *Report from Working Group 4: Opportunities in Flavour Physics at the HL-LHC and HE-LHC*, *CERN Yellow Rep. Monogr.* **7** (2019) 867 [[1812.07638](#)].
- [83] CMS collaboration, *Test of lepton flavor universality in $B^\pm \rightarrow K^\pm \mu^+ \mu^-$ and $B^\pm \rightarrow K^\pm e^+ e^-$ decays in proton-proton collisions at $\sqrt{s} = 13$ TeV*, [2401.07090](#).